CHAM

PHOENICS - Your Gateway to Successful CFD

PHOENICS NEWS

Editorial

Winter 2011

Since the last Newsletter was circulated Professor Spalding visited Melbourne Australia to participate in the 9th Australian Heat and Mass Transfer Conference held at Monash University.

His lecture referred to the population theory of computational fluid dynamics which was first raised, by him, in his Franklin lecture in April 2010 and is about to be published by the ASME.

We have passed the 30th anniversary of PHOENICS and are now intent on improving and expanding the code as we head for the 35th and 40th birthdays.

We wish all PHOENICS Users, present, past and future, a successful and enjoyable 2012.

2) News

2.1   PHOENICS News

2.1.1   PHOENICS 2012

Information regarding PHOENICS 2012 will appear in the next issue of the PHOENICS Newsletter. PHOENICS 2012 will feature Unstructured PHOENICS.

USP, as implied, uses an unstructured grid which means, in effect, that different grids can be used for different variables. The user must give additional instructions regarding the grid which is to be used but the result is appreciable computational economy.

It will also feature:
1. Improved residual calculation;
2. Improved cut-cell wall functions including low-Reynolds number turbulence models;
3. Improved sunlight model which can use EPW weather files;
4. Plotting on an arbitrary surface.

2.1.2 PHOENICS 2011
by John Ludwig, CHAM Limited

The changes listed below are those which have been incorporated into the code currently being distributed – PHOENICS 2011.

Editor:
1) Import group CAD objects and groups of CAD objects direct from the VRE menu.
2) Extend range of earth monitoring settings available from dialog.
3) Depth effect & Window size saved to the Q1 file
4) VR object names extended to 12 characters not 8.
5) Activation of transient restart made simpler
6) For ASSEMBLY objects, retain relative rotation angles of components relative to parent.
7) WIND object displays a blue arrow to show North and a red arrow to show the wind direction.
8) Correction to location of object 'at end' or 'to end' when also rotated.
9) Proto-type SUNLIGHT option added to WIND object. User inputs time of day, latitude, solar radiative flux, and heating is applied to faces of exposed objects.
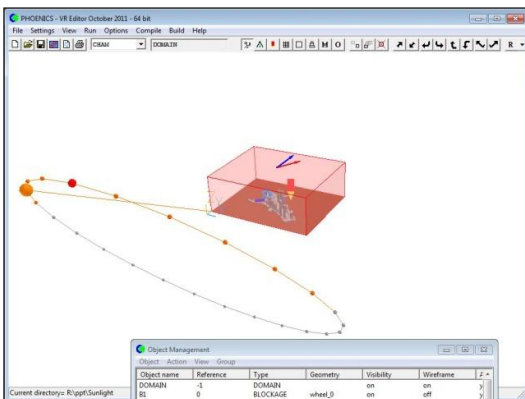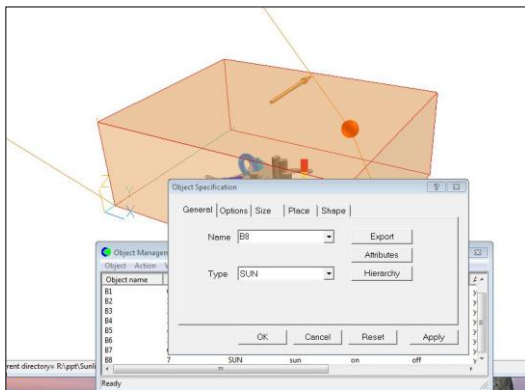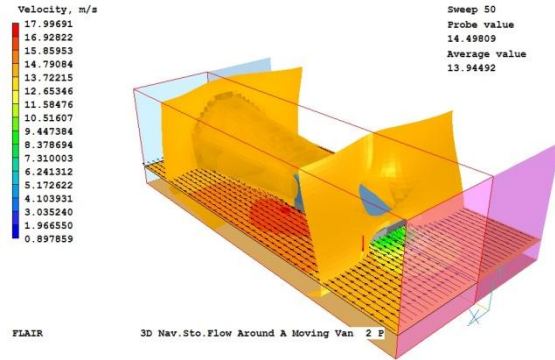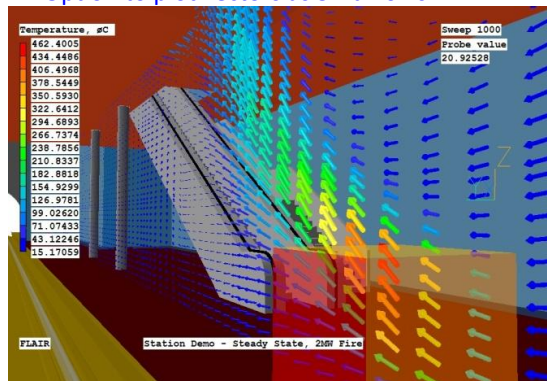
PIL:
1) PIL SUBROUTINEs can now be held in files which are accessed via INCL() statements.
2) New PIL command EXEC to execute named batch or other executable file when processing Q1.
3) New PIL command WRITE to write to a named file when processing Q1.

Viewer:
1) Option to mirror VR domain along symmetry plane.

2) Option to plot vectors as 3D arrows

3) F9 shortcut key added to load last saved phi file

Editor & Viewer:
1) Maximise window on start up, either through program argument or Q1 setting
2) Adjustment in near plane settings to help prevent domain being obscured when opening saved cases
3) Selectability status added to individual objects via object management panel
4) Set initial directory when opening the Change Directory dialog
5) Clipping plane is optionally applied to grid or results plotting plane.

Earth:
1) Earth monitor line width now variable. Default width set in CHAM.INI
2) Save record of last dumped phi file
3) Parallel restarts now possible from PHIDA files
4) When switching between monitor plot types the whole of the plot is redrawn enabling mutliple plots to be drawn at the end of a run.
5) Improvements to the new parsol detection, particularly for parallel runs.

6) PHOE_WORK_DIR environment variable use to modify the working directory of the compute nodes in parallel operation.
7) Result file now written for all compute nodes in parallel operation.
8) Correction to GCV multi-block links.
9) Correction to GENTRA transient restart.
10) Corrections to HOL to allow transient restart.
11) Corrections to parallel Earth interrupt screen to allow resetting of LSWEEP and maximum increment as in sequential.
12) In parallel send all time-history plots to result file of master processor to be picked up by Viewer.
13) HOL used same variables to control update frequency as already used for dumping frequency. Fixed by using separate controls.
14) Problem with SEM and temperature solution fixed
15) Correction to fully-rough wall function when roughness height < half near-wall cell height.
16) Problem with quadratic pressure boundary fixed

Flair:
1) SPRAYHEAD injection can start automatically when trigger temperature exceeded

InForm:
1) Correction to InForm to allow it to set source of VFOL in SEM.
2) InForm TABLE error limiting the table to two columns fixed
3) New command NETS to get nett source of a variable at an object
4) Problem with InForm source in transient when time limits of source fall outside scope of current run
5) Crash after field dump when more than one PWLF source fixed. Crash when more than 18 PWLF sources fixed. Reading of PWLF files more efficient.
6) Limit of characters on object/patch name when setting conductivity (prndtl(tem1)) raised to 8.

All:
Expiry Warning message occurs approximately 5 days before unlocking is due to expire.

2.2 Agents

Staff at Chemtech Brazil

3) PHOENICS Applications

3.1 CHAM Applications
Modelling of Data Centres
from a presentaton by Paul Emmerson, CHAM Limited

Modelling of data centres is a growing business for CHAM consultancy in UK and currently accounts for some 25% of all consultancy business. CHAM is the preferred supplier for certain data centre companies and models their major centres worldwide as well as working closely with their mechanical design sub-contractors.

Modelling is performed on new builds or developing existing data centres ie replacing low power computing with high density units to reduce footprint.
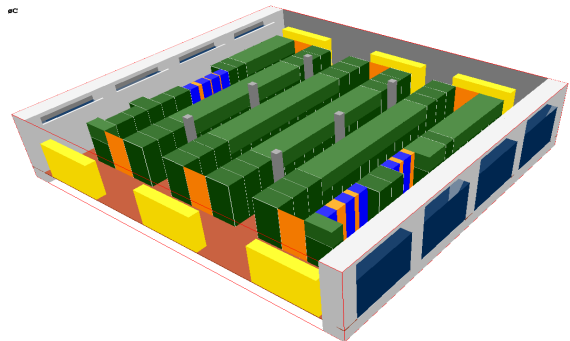

Figure 1: Data Centre

Types of Simulaton include:
1) Steady-state modelling for normal operation to:
• validate and test conceptual design
• help analyse and optimise the design environment
• Investigate cold/hot aisle containment systems
• assist with balancing and optimisation of chilled air flows/distribution
2) Steady-state modelling for CRAC failure scenarios:
• Data centres are designed for redundancy of air conditioning units (CRACs), and during maintenance these are carefully selected to reduce problems, but what if two or more were to fail in one region?
3) Transient modelling for power failure scenarios:
• Data centres are designed with a UPS system to ensure continuous operation of computers in the event of a power failure, but cooling systems rely on backup systems (e.g. diesel generators)
• Diesel generators will take several minutes to come on line and return full cooling capacity but heat input from computers & other sources will continue
• What happens to air temperatures during this period?

CHAM's advantages include:
1) Streamlined system for setting up data centres based on an approach which uses a spreadsheet to hold information about all components in the data centre, linked to a parameterised Q1 taking this information and automatically building the objects. This allows a fast and cost-effective service.
2) Data centre modelling can be fully customised to meet clients requirements which usually take the format of supplying chilled air into an under-floor plenum, and

then through perforated floor tiles to enable effective cooling of rack mounted computers.

CHAM has modelled unusual formats, for example where there were three floors of computer components with ventilation air allowed to pass between each floor through grilles.

Further information on this application is available from CHAM.

3.2 User Applications

3.2.1 Modelling of Solid-Liquid Slurry Flows in Horizontal Pipes
by Gianandrea Messa, Polytechnic School of Milan, Italy

Introduction

Investigations of solid-liquid slurry flows in industrial plants are being performed by the research group of Prof. Stefano Malavasi at the Hydraulic Section of Department I.I.A.R. of Polytechnic School of Milan. Solid-liquid slurry flows are encountered in many applications in civil & industrial engineering. Knowledge of their behavior is fundamental to ensure correct and efficient functioning of plants. In fact, the presence of solid particles in a liquid flow may produce undesirable events such as the increase in head losses, the damage to security devices, and the erosion of the ducts.

Flow of solid-liquid mixtures is very complex and the development of accurate models for its descriptions is one of the most important concerns of researchers. The solid-liquid slurry flow in a horizontal pipe is studied numerically using PHOENICS. Results are compared to experimental data available in literature [6].
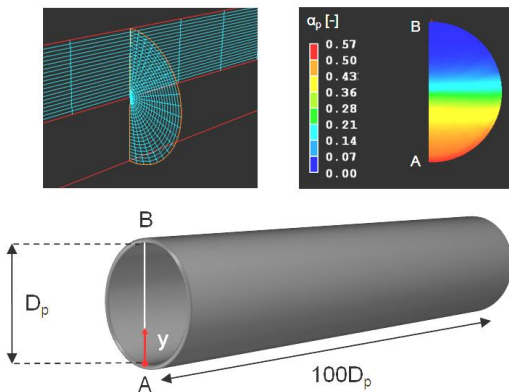

Figure 1. Sketch of the problem

Numerical model

The basic flow conditions of the present work are among those considered by Roco and Shook [6], who performed an investigation of the flow of slurries through horizontal pipes. Pipe diameter D_p is 51.7 mm, mean velocity of both phases is 3.44 m/s and the mean solid volume fraction is $\bar{\alpha}_p = 0.2034$. The carrier fluid is water (density $\rho_C = 998.23$ kg/m^3; kinematic viscosity $\nu_C = 10^{-6}$ m^2/s), the solid phase is sand with particle diameter $d_p = 480$ μm and density $\rho_p = 2645$ kg/m^3.

The two-phase problem was studied by means of the IPSA model available in PHOENICS. To correctly reproduce the phenomenon, the model has been customized with respect to the following aspects:

- Drag force: the drag force correlation for dispersed flows has been used. The drag coefficient is derived from the correlation of Ishii and Mishima [3]:

$$C_d = \begin{cases} \dfrac{24}{R_p}\left(1 + 0.1 R_p^{0.75}\right) & R_p < 1000 \\[3mm] 0.45\dfrac{1 + 17.67\left[\sqrt{1-\alpha_p}\left(\dfrac{\mu_C}{\mu_m}\right)\right]^{6/7}}{18.67\sqrt{1-\alpha_p}\left(\dfrac{\mu_C}{\mu_m}\right)} & R_p > 1000 \end{cases}$$

where the particle Reynolds number R_p is defined with respect to the viscosity of the mixture ν_{mix}, and, therefore, is equal to $d_p\left|\vec{U}_s\right|/\nu_{mix}$, $\vec{U}_s = \vec{U}_p - \vec{U}_C$ being the difference between the velocity of the dispersed and continuous phase. The mixture viscosity ν_{mix} is evaluated by means of the formula of Ishii and Mishima [3]:

$$\nu_{mix} = \nu\left(1 - \frac{\alpha_p}{\alpha_{p,\max}}\right)^{-2.5\alpha_{p,\max}} \quad (1)$$

in which $\alpha_{p,\max}$ is the maximum packing particle volume fraction, assumed equal to 0.62.

- Viscous stresses in the solid phase: the viscous stress in the solid phase is modeled by a Newtonian stress-strain constitutive relation, with the viscosity of the solid phase ν_p derived from that of the mixture ν_{mix} (Eq. (1)) by means of this linear weighted relation:

$$\nu_{mix} = \alpha_p \frac{\rho_p}{\rho_C}\nu_p + (1-\alpha_p)\nu \quad (2)$$

- Reynolds stresses: the Reynolds stress tensor of both phases is modeled by a Boussinesq assumption. The eddy viscosity of the continuous phase ν^T is derived by the *k*-ε turbulence model, while that of the solid phase ν_p^T by the Hinze Tchen [2] algebraic turbulence model:

$$\frac{\nu_p^T}{\nu^T} = \left(1 + \frac{\tau_p}{\tau_C}\right)^{-1} \quad (3)$$

where τ_C is the turbulent time scale of the continuous phase and τ_p the response time of the solid phase, in turn given by:

$$\tau_C = 1.22 C_\mu^{3/4} \frac{k}{\varepsilon} \quad (4)$$

$$\tau_p = \frac{\rho_p d_p^2}{18\rho_C \nu(1 + 0.15 R_p^{0.687})} \quad (5)$$

k being turbulent kinetic energy, ε its dissipation rate and C_μ equal to 0.09.

- Wall boundary conditions: at the pipe wall, the standard log law was applied to the continuous phase, while the following Bagnold-type shear stress (Matousek [5]) is imposed to the solid phase:

$$\tau_{W,p} = 0.00002\rho_p \left[\left(\frac{\alpha_{p,\max}}{\alpha_p} \right)^{1/3} - 1 \right]^{-2} |U_p|\overline{U}_{W,p} \quad (6)$$

- Wall force: the following wall-force term (Antal *et al.* [1]) is introduced in the momentum equation of both phases to account for the interactions between the particles and the pipe wall:

$$\vec{M}_p^W = -\vec{M}_C^W = \frac{2\alpha_p\rho_C |U_s^{//}|^2}{d_p} \left[C_{W1} + C_{W2}\left(\frac{d_p}{2y_0}\right) \right]\vec{n}_W$$

$$(7)$$

in which $U_s^{//}$ is the component of the slip velocity parallel to the wall, y_0 the distance between the cell and the wall, and $\vec{n}_W$ the outward normal vector on the surface of the wall, and C_{W1} and C_{W2} numerical constants, assumed equal to -0.2 and 0.24 respectively.

Results

Figure 2 shows the solid volume fraction profile along the vertical diameter (AB in Fig. 1). The good agreement between the numerical predictions and the experimental data of Roco and Shook [5] indicates that the model seems to be suitable to reproduce the phenomenon. In particular, the definition of the particle Reynolds number with respect to the mixture viscosity and the introduction of a specific turbulence model for the solid phase was found to be fundamental when dealing with highly concentrated slurries.
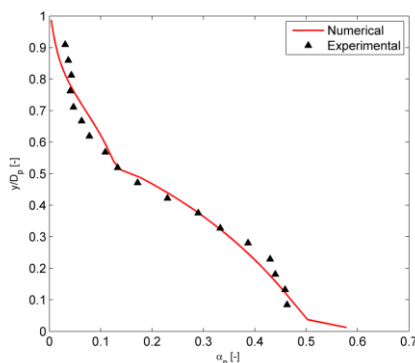

Figure 2. Solid volume fraction profile along the vertical diameter (AB in Fig. 1).

Figure 3 reports the axial velocity of both phases along the vertical diameter (AB in Fig. 1). The profiles are asymmetric, with the maximum velocity above the centerline of the channel. This behavior, observed also by other Authors (Ling *et al*. [4], Wei and Liejin [7]) can be explained considering that the slurry density near the pipe bottom is higher than that in the upper part due to the effect of gravity. This, in turn, may lead to a higher resistance to the motion of the slurry and therefore to a lower mixture velocity in this area.
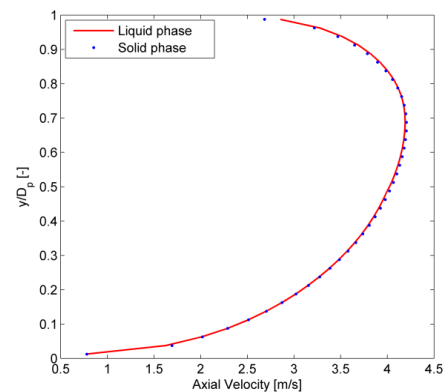

Figure 3. Axial velocity distribution along the vertical diameter (AB in Fig. 1) for the two phases. $\quad (7)$

References

1. Antal, S.P., Lahey Jr, R.T., Flaherty, J.E. (1991). Analysis of phase distribution in fully-developed laminar bubbly two-phase flow. *Int. J. Multiphase Flow* **17(5)**, 635-652.
2. Chen, X., Li, Y., Niu, X., Li, M., Chen, D., Yu, X. (2011). A general two-phase turbulent flow model applied to the study of sediment transport in open channels. *Int. J. Multiphase Flow* **37(9)**, 1099-1108.
3. Ishii, M., Mishima, K. (1984). Two-fluid model and hydrodynamic constitutive relations. *Nuclear Engineering and Design* **82(2-3)**, 107-126.
4. Ling, J., Skudarnov, P.V., Lin, C.X., Ebadian, M.A. (2003). Numerical investigations of solid-liquid slurry flows in a fully developed flow region. *Int. J. Heat and Fluid Flow* **24(3)**, 389-398.
5. Matousek, V. (2005). Research developments in pipeline transport of settling slurries. *Powder Tech.*, **156(1)**, 43-51.
6. Roco, M.C., Shook, C.A. (1983). Modeling of Slurry Flow: The Effect of Particle Size. *Canadian J. Chem. Eng.* **61(4)**, 494-503.
7. Xiaowei, H., Liejin, G. (2010). Numerical investigation of catalyst-liquid slurry flow in the photocatalytic reactor for hydrogen production based on algebraic slip model. *Int. J. Hydrogen Energy* **35(13)**, 7065-7072.

3.2.2 Evaluation of Nitric Oxide Reduction due to a Flue Gas Recirculation using PHOENICS-2008 by

S G Kobzar & A A Khalatov
Institute of Engineering Thermophysics, National Academy of Sciences, Kiev, Ukraine

Abstract

The investigation of a nitric oxide reduction by means of the flue gas recirculation technique was carried out. As found, for the Ukrainian DKVr 4/13 boiler supplied with GMG-2 burners the optimal flue gas recirculation ratio is observed between 15% and 20%.

The Objective

This research goal is to determine influence of the flue gas amount (the recirculation ratio) in the combustion air on a nitric oxide reduction in a boiler furnace and determination of an optimum magnitude of the recirculation ratio providing the lower level of the nitric oxide at the acceptable pressure drop and mass

flow rate of an air and flue gas mixture. The analysis showed the Ukrainian boilers of DKVr design, in particular a DKVr 4/13 boiler are the mostly applicable to implement the flue gas recirculation technique in the industrial and municipal sector.

The Object and Approach

The boiler DKVr 4/13 has two gas-oil burners GMG-2.0. The air supplied is divided into two different streams, where 10% of the primary air is going to the central circular hole. The primary air section is equipped with swirler having a swirl flow parameter of 0.9. The natural gas supplies through the annular duct located between the primary and secondary air sections. The secondary air section has a swirler with the swirl flow parameter of 1.6.

The investigation was carried out using *PHOENICS*-2008 software. As the basic combustion process occurs in a boiler furnace, the nitric oxide calculations were arranged using the boiler furnace model, built in a preprocessor VR Editor based on the Cartesian coordinate system.

To calculate the velocity, concentration and temperature fields the averaged Reynolds equations of the momentum and energy saving in the form of an enthalpy were used and solved. The *RNG k - ε* model providing the best results for a swirl flow was used. The radiant heat flow was calculated using the *Radiosity* model [1]. The furnace walls blackness was constant and equal to 0.9. The tubes surface temperature inside a furnace was constant and equal to $194^{o}C$ that is the water boiling temperature at the excessive water pressure of 13 MPa.

To simulate the natural gas combustion in a DKVr boiler furnace the two-stage mechanism of methane combustion [2] was used, as show below:

$$CH_4 + \frac{3}{2}O_2 \rightarrow CO + 2H_2O$$

$$CO + \frac{1}{2}O_2 \rightarrow CO_2 \qquad (1.1)$$
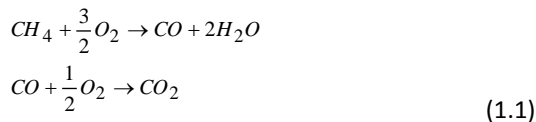
The average speed of the first reaction was determined by means of an Eddy Break Up model (*EBU)* [3] where C_{EBU} is 2.0: $\qquad (1.2)$

$$R_{CH_4} = -C_{EBU} \cdot \min\left(CH_4; \frac{O_2}{3,0}\right) \cdot \rho \frac{\varepsilon}{k} \; [kg/(m^3s)]$$

The average speed of an CO to CO_2 oxidation was determined as the minimal magnitude of the reaction speed according to an EBU model and Arrhenius law:

$$R_{CO} = - \min (R_{EBU}, R_{Ar}), \qquad (1.3)$$

where:

$$R_{Ar} = 5.4 \cdot 10^9 \exp\left(-\frac{15000}{T}\right)[CO][O_2]^{0.25}[H_2O]^{0.5}$$

[kmole/(m3·s)]. The nitric oxide emission formation was carried out taking into consideration the *Thermal* and *Prompt* mechanisms [4-7]. Thus, it was considered that NO_x has molecular mass M_{NO} of 30.

The Influence of a Flue Gas Recirculation on a Nitric Oxide Formation

Basic variant. As the first stage, a DKVr 4/13 boiler furnace operation was analyzed at the nominal operation conditions without a flue gas recirculation. All burners were operated at the excess-air coefficient ⬛⬛ of 1.15, the total fuel rate *G* was 0.0912 kg/s that is corresponding to the boiler thermal power of 4 MWt and the efficiency of 90 %. The basic results for this variant are shown in Fig. 1 – 3; all presented data were obtained in the horizontal cross-section cutting through the burner axis.

The hydrodynamics of a DKVr 4/13 boiler furnace demonstrates the complex and three-dimensional flow inside the furnace (Fig. 1). The swirling flow coming out from two burners forms the back-flow zone over each burner axis. Also, the enhanced turbulence generation is observed in the back-flow zone influencing greatly on the fuel-air mixing process and fuel combustion. This conclusion is confirmed by the temperature field results presented in Fig. 2. The joint operation of two burners forms two separate torches each around 1.5 m long.
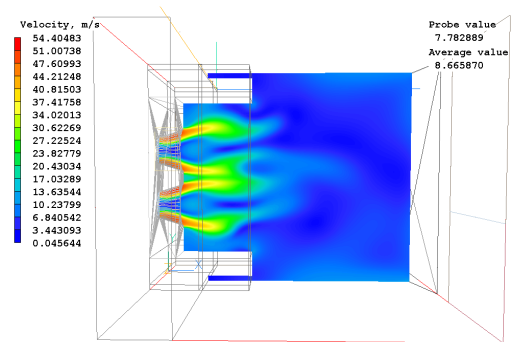
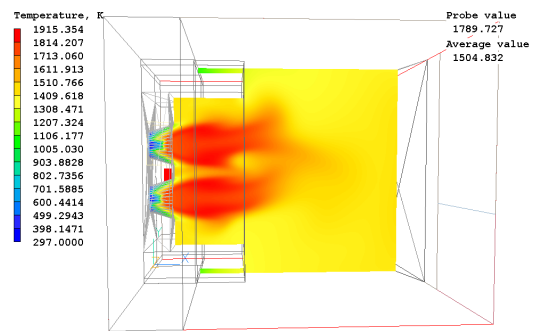

Fig. 1 The velocity field.

Fig. 2 The temperature field.

The analysis of the fuel concentration field showed the primary fuel portion burns down at the distance of 0.5 m from the burner outlet, while the carbon oxide combustion process completes at the distance of 1.2 m from the burner outlet. Results presented in Fig. 3 showed the primary amount of the nitric oxide is formed in the area close to each burner axis (high temperature zone), but after that they are spread throughout the furnace space due to effect of the vortex flow.

Distribution of the volume rate of the nitric oxide formation according to the Thermal and Prompt mechanism showed that basic contribution to the nitric oxide formation provides a Thermal mechanism. However one possible to distinguish two different zones of maximal nitric oxide formation; the first (primary) zone locates on the border between the secondary air and fuel motion, while the other one locates on the burner axis at the distance around of one diameter of the burner primary air path.
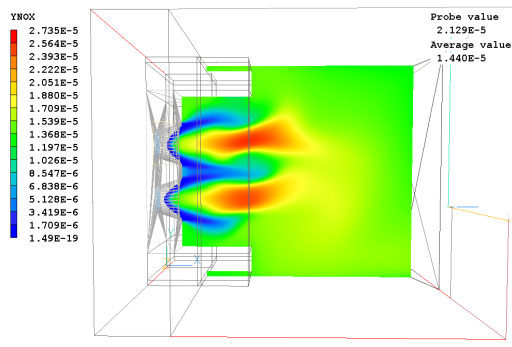

Fig. 3 – The nitric oxide concentration field.

By integrating calculation results at the furnace exit, the following results were obtained for the basic variant: CO concentration is 5.94 mg/nm^3; NO$_x$ concentration is 166 mg/nm^3; maximum temperature in the furnace T_{max} is 1915 K; required pumping pressure P is 700 Pa. The basic variant results were then used as the reference data when studying the flue gas recirculation on the boiler ecological characteristics. These results were also employed to summarize the data obtained for different variants of combustion products recirculation.

Effect of a flue gases recirculation. Analysis of basic variant data led to a conclusion to study two different ways of combustion products recirculation. The first way is based on the uniform diluting of the combustion air (uniform recirculation) by a flue gas, while the second one includes a flue gas supply into the burner secondary air duct (recirculation into a secondary air). For both cases calculations were carried out at various ratio of a flue gas recirculation. The flue gas temperature was 180°C, the mass concentration of chemical compounds in the primary and secondary air was recalculated taking into account their concentration in a flue gas and a flue gas amount used for recirculation.

Results characterizing the temperature and nitrogen oxide concentration fields for 20% uniform recirculation ratio are presented in Fig. 4 and Fig. 5. Analysis of these results shows for various ways of a flue gas supply the flow structure does not change radically, but the local temperature peak reduction is more observed for the uniform recirculation case.

As found, the reduction in the nitrogen oxide discharge is attained due to decrease in the local temperature peaks. Figure 6 shows the maximal temperature change in a furnace as a function of a flue gas recirculation ratio. As seen from this figure, for the uniform recirculation case the growth in recirculation ratio by 10 % leads to decrease in the maximum flow temperature of about 50 degrees. In case of recirculation of a flue gas into a secondary air the decrease in the maximum temperature is about 35 degrees for each 10% of a flue gas recirculation ratio. Reduction in local temperatures leads to decrease in the nitric oxide formation according to the Thermal mechanism, which brings the primary contribution to the total amount of the nitric oxide at the natural gas burning. The relationship between decrease in a nitrogen oxide level and a flue gas recirculation ratio is presented in Fig. 7. This data show when using the flue gas recirculation there is a good opportunity to reduce the nitric oxide discharge up to 80%.
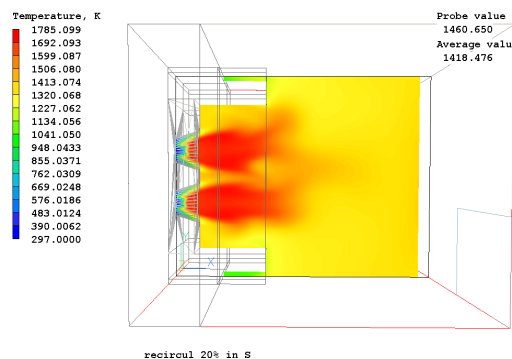

recircul 20% in S

Fig. 4   The temperature field (recirculation ratio is 20 %).
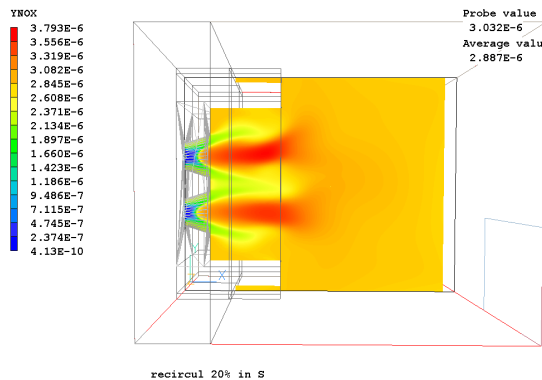

recircul 20% in S

Fig. 5   The nitrogen oxide concentration field (recirculation ratio is 20%).
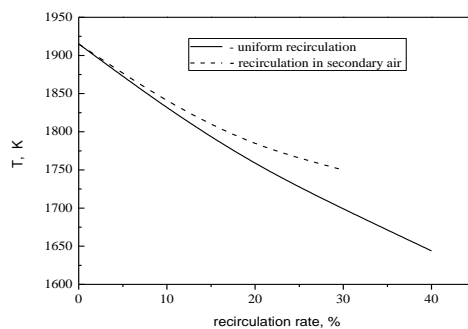

Fig. 6   The relationship between maximal temperature in a boiler and the flue gas recirculation ratio.

Figure 7 data confirm the chance to reduce the nitric oxide discharge by using the flue gas recirculation technique however this does not allow assessing the flue gas recirculation ratio. To provide the optimization analysis, the results of pressure drop, emission of carbon and nitrogen oxide were normalized by using the reference data obtained for the basic boiler variant (ΔP_0, NOx_0, CO_0). The results of such a summarizing are presented in Fig. 8. The data presented in Fig. 8 allow drawing a conclusion that optimal value of the flue gas recirculation ratio for a DKVr 4/13 boiler (burners GMG-2) is observed between 15% and 20%. This recirculation ratio provides decrease in the nitric oxide emission by 50…70 % at increase in the pressure providing the required air flow rate through burners by 20…30%. The further increase in the flue gas recirculation rate leads to a slight decrease in the nitric oxide at the substantial growth in the pressure required to pump an air.

There is a limiting magnitude of the flue gas recirculation ratio (35…40 %), at which the recirculation technique can be successfully applied. After 40% of the flue gas recirculation ratio, the oxygen in air flow mass fraction which is going for a combustion process becomes less than 17%, leading to a deterioration conditions for combustion. The growth in the carbon oxide testifies about it.
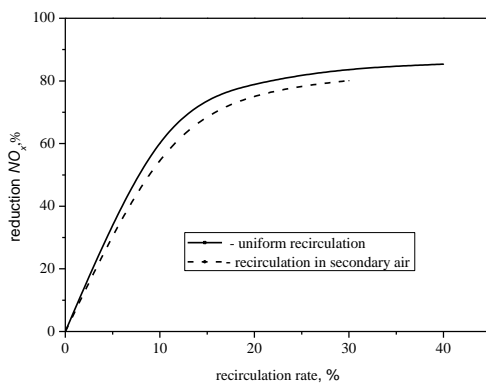

Fig. 7 The nitrogen oxide reduction as a function of a flue gas recirculation ratio and the way of its recirculation.
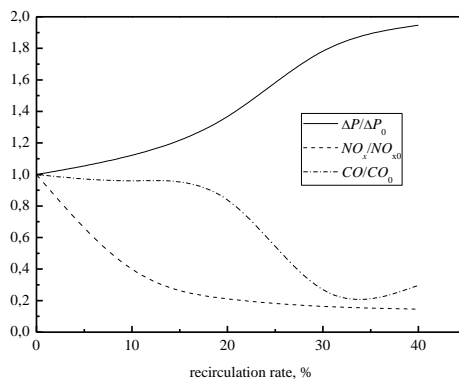

Fig. 8 The relationship between basic parameters of a DKVr 4/13 boiler and the flue gas recirculation ratio at the uniform recirculation.

Conclusions

The investigation of two different ways of a flue gas recirculation in a DKVr 4/13 boiler equipped with GMG - 2 burners shows:

- The uniform dilution of combustion air by a flue gas demonstrates slightly better effect on the decrease in the nitric oxide level;
- The optimal magnitude of the flue gas recirculation ratio is observed between 15% and 20%. In this case the decrease in the nitric oxide is from 50% to 70 %, while increase in the pressure required for the blast mixture pumping is between 20% to 30 %;
- After 40% of the flue gas recirculation ratio, the oxygen amount in a flow going for combustion becomes below 17 %, that deteriorates conditions for fuel combustion.

References

1. PHOENICS Reference Guide Version 3.6. CHAM, London – 2004.
2. *A. Khalatov, S. Kobzar, G. Kovalenko & V. Demchenko.* Thermogasdynamics and Ecological Characteristics of a Boiler Combustion Chamber Using Natural Gas // The 11th PHOENICS Users Conference, London, UK, 2006.
3. *D. Spalding* Mixing and Chemical Reaction in Steady Confined Turbulent Flames. In 13th Symp. (Int.) on Combustion, p. 649– 657, Pittsburgh, 1971. The Combustion Institute, Pittsburgh.
4. *Ya. Zel'dovich, G. Barenblatt, V. Librovich, & G. Mahviladze*. Mathematical Theory of Combustion and Explosion.- Moscow: Nauka (Publishers).-1980.-478 p.
5. *A. Williams, A. Clarke, & M. Pourkashanian.* The Mechanism of NO_x Formation During Combustion of Coal. NO_x Generation and Control in Boiler and Furnace Plant Symposium, 8th September. Portsmouth.-1988.
6. *G. De Soete.* Overall Reaction Rates of NO and N_2 Formation From Fuel Nitrogen, 15th Symp. (Int.) on Combustion. The Combustion Institute. – 1975, pp. 1093-1102.

4) PHOENICS Courses

CHAM holds regular PHOENICS Training Courses at its Head Office in Wimbledon Village, London. Courses can also be held at client premises by arrangement with Peter Spalding (pls@cham.co.uk).

The next courses are scheduled for:
24-26 January 2012
27-29 March 2012
29-31 May 2012 (provisional)

To contribute to any edition of the PHOENICS Newsletter please send technical articles, news items, photographs, course and meeting details, or any other items of interest to Colleen King (cik@cham.co.uk).